Interactions among Membrane and Soluble Components of the Flagellar Export Apparatus of *Salmonella*[†]

Keng Zhu, Bertha González-Pedrajo, and Robert M. Macnab*

Department of Molecular Biophysics and Biochemistry, Yale University, New Haven, Connecticut 06520-8114

Received May 1, 2002; Revised Manuscript Received June 7, 2002

ABSTRACT: Interactions among several components of the flagellar export apparatus of *Salmonella* were studied using affinity chromatography, affinity blotting, and fluorescence resonance energy transfer (FRET). The components examined were two integral membrane proteins, FlhA and FlhB, and two soluble components, FliH and the ATPase FliI. Affinity chromatography and affinity blotting demonstrated a heterologous interaction between FlhA and FlhB but not homologous FlhA−FlhA or FlhB−FlhB interactions. Both FlhA and FlhB consist of N-terminal transmembrane domains and C-terminal cytoplasmic domains ($FlhA_C$ and $FlhB_C$). To study the interactions among the cytoplasmic components ($FlhA_C$, $FlhB_C$, FliH, and FliI), FRET measurements were carried out using fluorescein-5-isothiocyanate (FITC) as donor and tetramethylrhodamine-5- (and 6-) isothiocyanate (TRITC) as acceptor. To reveal the nature of the binding interactions, measurements were carried out in physiological buffer, at high salt (0.5 M NaCl) and in 30% 2-propanol. The results indicated that $FlhA_C$ could bind to $FlhB_C$ and both $FlhA_C$ and $FlhB_C$ could bind to themselves. Both $FlhA_C$ and $FlhB_C$ bound to FliH and FliI. Several in-frame deletion mutants of FliH were examined and found to have only minor effects of decreased binding to $FlhA_C$ and $FlhB_C$; deletions in the interior of the FliH sequence had a greater effect than those at the N terminus. The FliI mutants examined bound $FlhA_C$ and $FlhB_C$ about the same as or slightly more weakly than wild-type FliI. FliH bound more weakly to FliI carrying the N-terminal double mutation R7C/L12P than it did to wild-type FliI, confirming the importance of the N terminus of FliI for its interaction with FliH.

The type III flagellar export apparatus of *Salmonella* is complex. It consists of six integral membrane components (FlhA, FlhB, FliO, FliP, FliQ, and FliR) in addition to some soluble components (FliH, FliI, the putative chaperone FliJ, and the specific chaperones FlgN, FliS, and FliT) (*1*−*9*). Except for the latter three, these proteins are general export components that are required for export of all substrates: rod-type proteins (FlgB, FlgC, FlgF, FlgG, and FliE), hook-type proteins (FlgD and FlgE), and filament-type proteins (FlgM, FlgK, FlgL, FliC, and FliD) (*4*, *5*). The membrane components are believed to be located in a central pore within the membrane−supramembrane or MS ring (*2*, *10*, *11*).

FlhA is a large integral membrane protein containing 692 residues. FlhB, also an integral membrane protein, is smaller, containing 383 amino acids. Both FlhA and FlhB have highly hydrophobic N termini and soluble C termini. The N termini of FlhA and FlhB are transmembrane domains with eight and four predicted spans, respectively (*12*−*14*). The C-terminal domains of both FlhA and FlhB ($FlhA_C$ and $FlhB_C$)[1] are predicted to be located in the cytoplasm and to be involved in substrate translocation and substrate specificity switching, respectively (*5*).

FliI is an ATPase whose enzymatic activity is essential for flagellar assembly (*1*). FliI has significant sequence similarity to the catalytic β subunit of the proton-translocating F_oF_1 ATPase (*15*), including well-conserved residues within the so-called Walker boxes. However, FliI has an N-terminal overhang of about 30 amino acids, which is lacking in the F_1 β subunit, and significant sequence similarity between the two proteins is not evident until around position 100 of the FliI sequence. These facts indicate that the N terminus of FliI has a flagellum-specific function: it was suggested that it might be responsible for interaction with other flagellar components and also for exerting a regulatory effect on the catalytic mechanism. The role of FliH is less clear. Minamino and Macnab found that FliH and FliI can form a heterotrimeric complex $(FliH)_2FliI$ and that the ATPase activity of the complex was about 10-fold lower than that of FliI alone (*16*); i.e., FliH appears to function as a negative regulator. The properties of FliI and the $(FliH)_2FliI$ complex in terms of proteolytic sensitivity suggest a hinge region between the flagellum-specific domain and the ATPase

[†] This work has been supported by USPHS Grant AI12202 and by a postdoctoral fellowship from Consejo Nacional de Ciencia y Tecnología (CONACYT) to B.G.-P.

* Address correspondence to this author at the Department of Molecular Biophysics and Biochemistry 0734, Yale University, P.O. Box 208114, 266 Whitney Ave., New Haven, CT 06520-8114. Phone: (203) 432 5590. Fax: (203) 432 9782. E-mail: robert.macnab@yale.edu.

[1] Abbreviations: FLAG, epitope for commercially available monoclonal antibody; $FlhA_C$ and $FlhB_C$, soluble cytoplasmic domains of proteins FlhA and FlhB, respectively; $FlhB_{CN}$ and $FlhB_{CC}$, soluble N-terminal and C-terminal subdomains of $FlhB_C$; $FlhA_{TM}$ and $FlhB_{TM}$, transmembrane domains of FlhA and FlhB, respectively; FITC, fluorescein-5-isothiocyanate; FRET, fluorescence resonance energy transfer; *i*PrOH, 2-propanol; IPTG, isopropyl β-D-thiogalactopyranoside; Ni-NTA, nickel nitrilotriacetic acid; PCR, polymerase chain reaction; SDS−PAGE, sodium dodecyl sulfate−polyacrylamide gel electrophoresis; TRITC, tetramethylrhodamine-5- (and 6-) isothiocyanate.

10.1021/bi0203280 CCC: $22.00
Published on Web 07/04/2002

domain (*17*). The central region of FliH is important for dimerization, the C-terminal region is important for interaction with FliI, and the N-terminal region may be responsible for interaction with the general chaperone FliJ (*18*).

On the basis of affinity blotting, the C-terminal cytoplasmic domain of FlhA ($FlhA_C$, residues 328−692) was found to bind substrates such as FlgD, FlgE, and FliC. It bound strongly to FliJ, moderately to FliH and FliI, and weakly to itself (*5*). The C-terminal cytoplasmic domain of FlhB ($FlhB_C$, residues 211−383) is unstable, being specifically cleaved by endogenous proteases between Asn269 and Pro270 into two polypeptides, which have been designated $FlhB_{CN}$ and $FlhB_{CC}$ (*14*). The interaction of $FlhB_C$ with the hook-length control protein FliK, rod- and hook-type substrates (FliE, FlgB, FlgE, and FlgD), and filament-type substrates (FlgK, FlgL, and FliC) has been studied by affinity blotting (*5*, *14*). $FlhB_C$ binds more strongly to rod- and hook-type substrates than to filament-type substrates. $FlhB_C$ somehow communicates with the C-terminal domain of FliK, resulting in substrate-specificity switching from rod- and hook-type substrates to filament-type substrates (*13*). It was proposed that $FlhB_C$ has two substrate-specificity states and that a conformational change, mediated by the interaction between $FlhB_{CN}$ and $FlhB_{CC}$, is responsible for the specificity switching process (*14*). After studying the soluble export components of the flagellar export apparatus and interactions among them and their substrates, Minamino and Macnab (*5*) suggested a tentative model for the type III flagellar export process. (i) First, a FliH−FliI−FliJ−substrate complex is formed in the cytoplasm, possibly from FliH−FliI and FliJ−substrate subcomplexes. (ii) This complex diffuses to the cytoplasmic domains of FlhA and FlhB and forms a $FlhA_C$−$FlhB_C$−FliH−FliI−FliJ−substrate complex at the central pore of the MS ring. (iii) ATP hydrolysis by FliI causes the substrate to be translocated across the plane of the cytoplasmic membrane through the transmembrane region of the export apparatus (FliO, FliP, FliQ, FliR, and the transmembrane domains of FlhA and FlhB) accompanied by dissociation of FliH, FliI, and FliJ from the export apparatus. (iv) Finally, the translocated substrate diffuses down the channel in the nascent structure and assembles at its distal end. Although the interactions of $FlhA_C$ and $FlhB_C$ with FliI and FliH have been studied (*5*), the experiments were not carried out in free solution. Also, the interactions between the full-length integral membrane components FlhA and FlhB were not examined.

In this paper, we have studied the interaction of full-length FlhA and FlhB using Ni-NTA affinity chromatography and affinity blotting. We have also used fluorescence resonance energy transfer (FRET) to study the interactions of the soluble domains $FlhA_C$ and $FlhB_C$ with wild-type and mutant versions of FliH and FliI.

EXPERIMENTAL PROCEDURES

Bacterial Strains, Plasmids, and Media. The plasmids used in this study are listed in Table 1. L broth (LB), soft tryptone agar plates, and M9-casamino acid medium were prepared as described previously (*4*). *Escherichia coli* NovaBlue (Novagen, Madison, WI) was used as the recipient in cloning experiments, and *E. coli* BL21(DE3)pLysS (Novagen) was used for overproduction of protein from pET- and pTrc-based plasmids.

Table 1: Plasmids Used in This Study

plasmid	relevant characteristics	source or reference
pMM106	pET19b/N-His-FLAG-FlhA	*12*
pMM130	pTrc99A/FlhA	*12*
pMK26	pTrc99A/FlhB (P270A)	this study
pMM102	pET19b/N-His-$FlhA_C$ (residues 328−692)	*5*
pMK10	pET19b/N-His-FlhB (P270A)	this study
pMM001	pET19b/N-His-$FlhB_C$ (residues 211−383)	*5*
pMM1701	pET19b/N-His-FliI	*5*
pIFF705	pTrc99A/N-His-FliI (R7C/L12P)	*1*
pIFF706	pTrc99A/N-His-FliI (K188I)	*1*
pIFF707	pTrc99A/N-His-FliI (K188E)	*1*
pIFF709	pTrc99A/N-His-FliI (Y363S)	*1*
pMM310	pET19b/N-His-FliH	*5*
pBGhHΔ1	pET19b/N-His-FliHΔ1 (1−10)	*18*
pBGhHΔ3	pET19b/N-His-FliHΔ3 (21−30)	*18*
pBGhHΔ4	pET19b/N-His-FliHΔ4 (31−40)	*18*
pBGhHΔ5	pET19b/N-His-FliHΔ5 (41−50)	*18*
pBGhHΔ6	pET19b/N-His-FliHΔ6 (51−60)	*18*
pBGhHΔ15	pET19b/N-His-FliHΔ15 (141−150)	*18*

PCR and Cloning. Synthetic primers containing restriction sites were synthesized using a model 393 DNA/RNA synthesizer (Applied Biosystems, Foster City, CA). PCR was carried out using an MJ minicycler (MJ Research, Watertown, MA) and Taq polymerase (Qiagen, Valencia, CA). PCR products were purified using a QIAquick gel extraction kit (Qiagen).

Culture and Lysis of Cells. Forty milliliters of overnight culture of BL21(DE3)pLysS cells carrying plasmids encoding untagged FlhA or FlhB or N-terminally His-tagged FLAG-FlhA, FlhB (P270A), $FlhA_C$, $FlhB_C$, FliI, or FliH was inoculated into 1 L of LB with ampicillin at 100 μg/mL and incubated at 37 °C with shaking until the cell density reached an optical density at 600 nm of 0.6−0.8. Then isopropyl β-D-thiogalactopyranoside (IPTG) was added to a final concentration of 0.2 mM, and incubation was continued for another 5 h. The cells were collected by centrifugation and stored at −20 °C. The cells were thawed and suspended in 80 mL of binding buffer and sonicated (model 450 sonifier, Branson Ultrasonics Corp.). The binding buffer used was 20 mM Tris-HCl and 500 mM NaCl, pH 8.0, for soluble proteins ($FlhA_C$, $FlhB_C$, FliI, FliH) and 50 mM Na_2HPO_4 and 0.1% Thesit, pH 7.9, for membrane proteins (FlhA, FlhB).

Preparation of Lysate Supernatants for Untagged FlhA and FlhB and Purification of His-Tagged Membrane Proteins FLAG-FlhA and FlhB (P270A). The cell lysates were centrifuged (20200*g*, 30 min, 4 °C) to pellet the membrane fraction, undisrupted cells, and inclusion bodies. This pellet was resuspended in 30 mL of extraction buffer (50 mM Na_2HPO_4, 500 mM NaCl, 1% Thesit, 4 M urea, pH 7.9), incubated at 4 °C with agitation for 1 h, and then centrifuged at 160000*g* for 1 h. The supernatant was separated into two parts, one for affinity chromatography and the other for purification. The sample for affinity chromatography was dialyzed against binding buffer with three changes. For purification, the sample was loaded onto a 3 mL Ni-NTA agarose column (Qiagen) preequilibrated with 9 mL of binding buffer (50 mM Na_2HPO_4, 0.1% Thesit, pH 7.9) and washed with 15 mL of buffer containing 25 mM imidazole. The proteins were eluted with 3 mL of buffer with 75 mM imidazole, 3 mL of buffer with 100 mM imidazole, 3 mL of buffer with 150 mM imidazole, and 3 × 3 mL of buffer with 250 mM imidazole.

Purification of N-Terminally His-Tagged $FlhA_C$, $FlhB_C$, FliI, and FliH. The cell lysates were centrifuged (20200*g*, 30 min, 4 °C) to pellet the membrane fraction, undisrupted cells, and inclusion bodies. The supernatant was centrifuged at 160000*g* for 1 h and the supernatant subjected to Ni-NTA chromatography as described above.

For the purification of N-His-$FlhA_C$, FliI, and FliH, the binding buffer was 0.5 M NaCl and 20 mM Tris, pH 8.0. For the purification of N-His-$FlhB_C$, the binding buffer was 50 mM Na_2HPO_4 and 0.1% Thesit, pH 7.9. We found that, in the absence of 0.1% Thesit, N-His-$FlhB_C$ did not bind to the column.

Ni-NTA Affinity Chromatography Assays. Solutions of the untagged and His-tagged proteins were mixed together and incubated at room temperature for 2 h with occasional shaking. The mixture was loaded onto a 3 mL Ni-NTA agarose column and eluted as described above.

Immunological Methods. To detect proteins, samples were separated by sodium dodecyl sulfate−polyacrylamide gel electrophoresis (SDS−PAGE), transferred to nitrocellulose membrane (Schleicher and Schull, Keene, NH), probed with the appropriate antibody, and then detected by enhanced chemiluminescence (Amersham International, Little Chalfont, U.K.) according to the manufacturer's instructions. The antibodies used were as follows: anti-$FlhA_C$ and anti-$FlhB_C$, gifts of K. Kutsukake (*19*); India HisProbe-HRP (Pierce, Rockford, IL); monoclonal anti-FLAG M2 (Sigma, St. Louis, MO); goat anti-rabbit HRP and goat anti-mouse HRP (Bio-Rad, Hercules, CA).

Affinity Blotting Analysis. After the target proteins had been separated by SDS−PAGE, they were transferred onto nitrocellulose membrane with a TE22 MiniTank TransPhor unit (Hoefer, San Francisco, CA). The membrane was blocked for 1 h with Tris-buffered saline/0.1% Tween 20/5% nonfat dry milk. After being washed with Tris-buffered saline/0.1% Tween 20, the membrane was soaked for 2 h in the same buffer plus 2 μg/mL purified probe proteins. The membrane was then probed with the appropriate antibody and immunodetection performed as described above.

Labeling of Proteins with FITC and TRITC. Soluble proteins were covalently labeled with the fluorescence probes fluorescein-5-isothiocyanate (FITC) and tetramethylrhodamine-5- (and 6-) isothiocyanate (TRITC) (Molecular Probes, Eugene, OR) according to the method of Koiv et al. (*20*). Before reaction with the probes, the proteins ($FlhA_C$, $FlhB_C$, FliI, or FliH) were dialyzed against sodium phosphate buffer, pH 9.5, to remove the Tris. A concentrated solution of either FITC (9 mM) or TRITC (10 mM) was added to the protein solution to yield a [fluorescent probe]/[protein] molar ratio of 5.0 for FITC or 10.0 for TRITC. The mixture was incubated for 3 h in the dark at room temperature with occasional shaking. The reaction was stopped by adjusting the pH of the reaction mixture to 6.0, and ca. 2.5−3 mL of the sample was dialyzed in cassettes (Pierce, Rockford, IL) against 300 mL of 0.6 M NaCl, 20 mM Hepes, and 0.1 mM EDTA, pH 7.0, to separate the unreacted fluorescent probes from the labeled protein. After 4 h, dialysis was continued against 20 mM Hepes buffer, pH 7.0, and 0.1 mM EDTA to remove the salt. The buffer was changed every 4 h, and the dialysis was continued until no fluorescence probe could be detected. Excitation/emission wavelength maxima for FITC and TRITC are 494/512 and 548/576 nm, respectively.

Table 2: Molar Label/Protein Ratios Achieved in This Study

protein	fluorescent probe	label/protein ratio	protein	fluorescent probe	label/protein ratio
$FlhA_C$	FITC	0.5	FliH	FITC	0.53
$FlhA_C$	TRITC	0.5	FliH	TRITC	0.45
$FlhB_C$	FITC	0.5	FliHΔ1	TRITC	0.42
$FlhB_C$	TRITC	0.56	FliHΔ3	TRITC	0.54
FliI	TRITC	4	FliHΔ4	TRITC	0.78
FliI (K188I)	TRITC	2.6	FliHΔ5	TRITC	0.82
FliI (R7C/L12P)	TRITC	2.8	FliHΔ6	TRITC	0.75
FliI (Y363S)	TRITC	2.5	FliHΔ15	TRITC	0.77

Protein concentration was determined using the D_C protein assay kit (Bio-Rad). The amount of FITC or TRITC bound to proteins was estimated by light absorbance at 499 and 544 nm using the molar extinction coefficients $\epsilon_{FITC} = 70000$ (*21*) and $\epsilon_{TRITC} = 84000$ (*22*), respectively. The label ratios of fluorescent probes for different proteins are given in Table 2.

Fluorescence Resonance Energy Transfer Measurements. Energy transfer measurements were carried out with a PTI Quantamaster C-61 spectrofluorometer (Photon Technology International, Ontario, Canada) equipped with a magnetically stirred, thermostated cuvette compartment. When FITC fluorescence intensity quenched by TRITC-labeled proteins was measured, the excitation wavelength was 494 nm and the emission wavelength varied from 512 to 518 nm, depending on the sample. Both excitation and emission bandpasses were 2 nm in all measurements. For fluorescence intensity measurements, errors were less than 0.5%. Where the TRITC/protein label ratio was <1 ($FlhA_C$, $FlhB_C$, and wild-type and mutant FliH, Table 2), the data were normalized to a ratio of 1, as follows: Let relative fluorescence intensity (unnormalized) = RFI and label ratio = LR. Then extent of quenching (unnormalized) = 1 − RFI, normalized extent of quenching = (1 − RFI)/LR, and normalized relative fluorescence intensity = [1 − (1 − RFI)/LR]. Normalization was not performed in the case of wild-type and mutant FliI, where the label ratio was >1. Also, since the extent of labeling with FITC was essentially constant, we did not normalize with respect to it.

ATPase Activity Measurements. The malachite green ATPase assay was performed as described previously (*16*). Fifteen microliters of purified N-His-FliI (0.5 $\mu g\ \mu L^{-1}$) was added to the ATP reaction buffer.

RESULTS

Interactions between Membrane Proteins of the Flagellar Export Apparatus Studied by Affinity Chromatography and Affinity Blotting. The full-length integral membrane proteins FlhA and FlhB(P270A) were used. The mutation Pro270 to Ala in FlhB was introduced because the wild-type protein is extremely sensitive to proteolytic cleavage at that position (*14*).

Interaction between FlhA and FlhB. When a His-tagged protein and an untagged protein are applied as a mixture to a Ni-NTA column, the untagged protein is often retarded if it forms a stable complex with the tagged one and is only eluted at relatively high imidazole concentrations (e.g., refs *16*, *18*, and *23*). We used this method to study the interactions

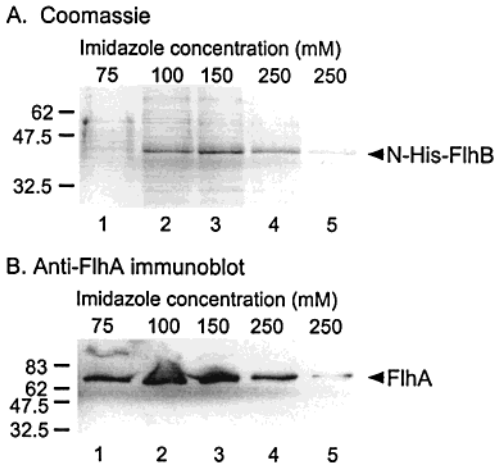

FIGURE 1: Test for FlhA−FlhB interactions using Ni-NTA affinity chromatography. Whole cell lysates of BL21(DE3)pLysS cells overproducing either N-His-tagged FlhB or untagged FlhA were mixed, applied to a Ni-NTA column, and eluted at the imidazole concentration indicated; lanes 4 and 5 represent two successive elutions at 250 mM imidazole. (A) Coomassie-stained gel. (B) Immunoblot using polyclonal anti-FlhA antibody. The positions of N-His-tagged FlhB and untagged FlhA are indicated to the right. Molecular mass standards are indicated to the left.

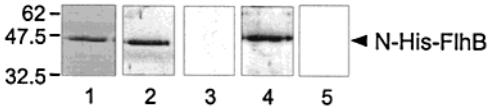

FIGURE 2: Affinity blotting of N-His-FlhB using purified N-His-FLAG-tagged FlhA as the probe. Lane 1: Coomassie-stained SDS−PAGE of overproduced N-His-FlhB (peak fractions from Ni-NTA chromatography). Lanes 2 and 4: affinity blotting of the sample in lane 1 probed with N-His-FLAG-FlhA and then probed with anti-FlhA (lane 2) or anti-FLAG (lane 4) antibody. Lanes 3 and 5: Immunoblotting of the sample in lane 1 probed directly with anti-FlhA (lane 3) or anti-FlAG (lane 5) antibody without prior incubation with FlhA.

between FlhA and FlhB. The supernatants containing untagged FlhA and N-His-FlhB, respectively, were prepared as described in Experimental Procedures. A mixture of N-His-FlhB and untagged FlhA in 50 mM Na_2HPO_4 and 0.1% Thesit (pH 7.9) at a molar ratio of about 1:1 was passed over a Ni-NTA column, washed with buffer, and then eluted with one column volume each of 75, 100, 150, and 250 mM imidazole. Coomassie-stained SDS−PAGE revealed that the peak fractions of N-His-FlhB were at 100, 150, and 250 mM imidazole (Figure 1A). Untagged FlhA (apparent molecular mass of ca. 70 kDa) could not be seen by Coomassie staining, but immunoblotting using polyclonal anti-FlhA antibody revealed its presence in the 75, 100, 150, and 250 mM imidazole fractions (Figure 1B). When untagged FlhA in the absence of N-His-FlhB was loaded onto the Ni-NTA column, it was eluted completely at 75 mM imidazole (data not shown). Thus the retardation of untagged FlhA is dependent on the presence of N-His-FlhB.

The interactions between FlhA and FlhB were also examined by affinity blotting (Figure 2). After purified N-His-FlhB had been subjected to SDS−PAGE (lane 1), the material was transferred to nitrocellulose membranes. These membranes were incubated for 2 h with N-His-FLAG-FlhA as a probe, and then immunoblotting was performed using either polyclonal anti-FlhA or monoclonal anti-FLAG antibodies. At the position of N-His-FlhB, N-His-FLAG-FlhA

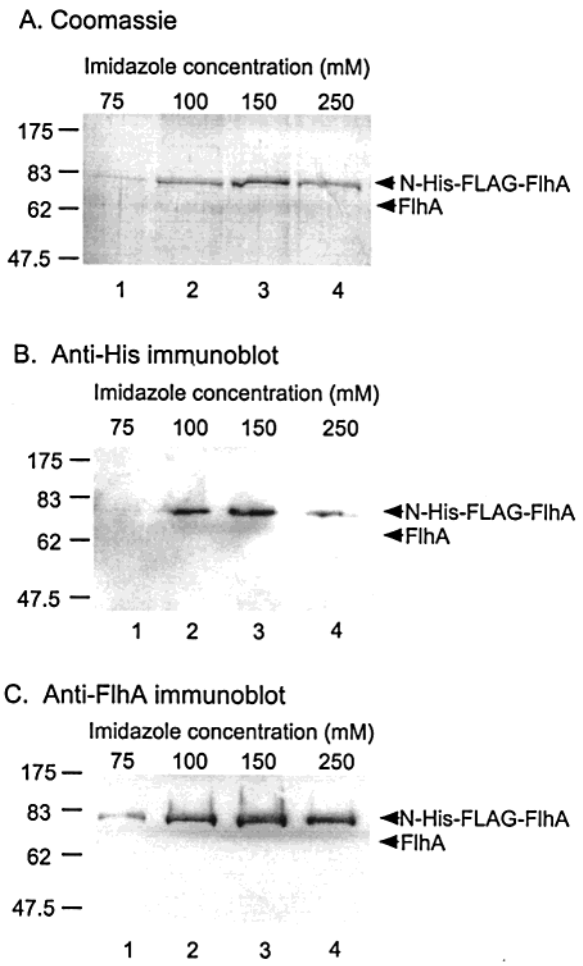

FIGURE 3: Test for FlhA−FlhA interactions using Ni-NTA affinity chromatography. Whole cell lysates of BL21(DE3)pLysS cells overproducing either N-His-FLAG-tagged FlhA or untagged FlhA were mixed and applied to a Ni-NTA column and eluted at the imidazole concentration indicated. (A) Coomassie-stained gel. (B) Immunoblot using monoclonal anti-His antibody. (C) Immunoblot using polyclonal anti-FlhA antibody. The position of N-His-FLAG-tagged FlhA is indicated to the right, along with (in gray) the approximate position expected for untagged FlhA if it were present. Molecular mass standards are indicated to the left.

could be detected by both anti-FlhA antibody (lane 2) and anti-FLAG antibody (lane 4). In membranes where the incubation with N-His-FLAG-FlhA was omitted, N-His-FlhB itself showed no cross-reaction with anti-FlhA antibody (lane 3) or anti-FLAG antibody (lane 5). Thus, these affinity blotting data confirm the finding from affinity chromatography, namely, that full-length FlhA and FlhB interact with each other.

Interactions of FlhA and FlhB with Themselves. A mixture of lysates of cells producing N-His-FLAG-FlhA and untagged FlhA was loaded onto a Ni-NTA column, washed with buffer, and then eluted with different concentrations of imidazole. At 100, 150, and 250 mM imidazole, a single band at about 75 kDa was detected by Coomassie staining (Figure 3A). Immunoblotting using anti-His (Figure 3B) or anti-FlhA antibody (Figure 3C) also revealed a single band at the same position. There was no indication of a second band at the position expected for untagged FlhA.

N-His-FlhB tends to degrade, making it difficult to use affinity chromatography to study FlhB−FlhB interactions. We therefore used affinity blotting. The lysates of *E. coli*

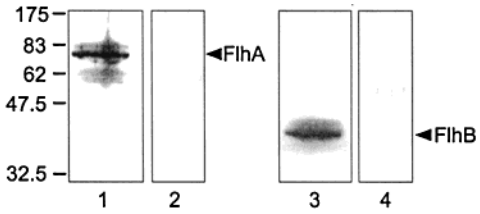

FIGURE 4: Test for homologous FlhA−FlhA and FlhB−FlhB interactions. Whole cell lysates were prepared of *E. coli* BL21(DE3)-pLysS cells, carrying plasmids pMM130 or pMK26, encoding untagged FlhA or untagged FlhB, respectively, and grown in the presence of 0.2 mM IPTG. Panel 1: Immunoblot of lysates of cells overproducing untagged FlhA, probed with polyclonal anti-FlhA antibody. Panel 2: Affinity blot of the same sample as in panel 1, probed first with N-His-FLAG-FlhA and then with anti-His antibody. Panel 3: Immunoblot of lysates of cells overproducing untagged FlhB, probed with polyclonal anti-FlhB antibody. Panel 4: Affinity blot of the same sample as in panel 3, probed first with N-His-FlhB and then with anti-His antibody. Molecular mass standards are indicated to the left.

BL21(DE3)pLysS cells with plasmids encoding untagged FlhA or untagged FlhB were subjected to SDS−PAGE, and the samples were transferred onto nitrocellulose membranes. These membranes were incubated for 2 h with N-His-FLAG-FlhA or N-His-FlhB, respectively, as probes, and then immunoblotting was performed with anti-His antibody. In neither case could His-tagged protein be detected (Figure 4, lanes 2 and 4). In control experiments, where probing with His-tagged proteins was omitted and immunoblotting was performed with polyclonal anti-FlhA and anti-FlhB antibodies, respectively, the presence of the untagged FlhA and FlhB proteins was readily detected (Figure 4, lanes 1 and 3). Thus neither affinity chromatography nor affinity blotting provided evidence for homologous FlhA−FlhA and FlhB−FlhB interactions (but see FRET data below).

Interactions of Soluble Proteins and Domains Studied by Fluorescence Resonance Energy Transfer (FRET). FRET is a widely used method for reporting the association of macromolecules (*24*, *25*). It has three preconditions: (i) There must exist a donor and an acceptor; (ii) the emission spectrum of the donor must overlap with the absorption spectrum of the acceptor; (iii) the distance between donor and acceptor should be less than about 7 nm (*26*). For technical reasons, FRET is not well suited for the study of integral membrane proteins. We therefore employed the soluble domains $FlhA_C$ and $FlhB_C$, as well as the soluble proteins FliI and FliH. Proteins were labeled with FITC and TRITC as donor and acceptor, respectively.

Interactions between $FlhA_C$ and $FlhB_C$. Interactions between $FlhA_C$ and $FlhB_C$ were studied by FRET using FITC-labeled $FlhB_C$ (FITC-$FlhB_C$) and TRITC-labeled $FlhA_C$ (TRITC-$FlhA_C$). Like full-length wild-type FlhB, $FlhB_C$ is unstable, being specifically cleaved at Pro270 (*14*). For our FRET measurements, we first tried to use the mutant domain $FlhB_C$ (P270A) but found that N-His-$FlhB_C$ (P270A) did not bind to a Ni-NTA column, perhaps because the His tag was occluded. Since $FlhB_{CN}$ and $FlhB_{CC}$ are known to stably interact with each other after cleavage (*14*), we therefore used wild-type N-His-$FlhB_C$ (effectively, N-His-$FlhB_{CN}$ + $FlhB_{CC}$) to study the interactions.

The emission spectrum of FITC-$FlhB_C$ (Figure 5A, spectrum 1) had a peak at 512 nm. With increasing amounts of TRITC-$FlhA_C$ (from 0 to 1.5 μM in 0.125 μM increments), the intensity at 512 nm decreased and a peak at 573 nm appeared with increasing intensity (spectra 2−13).

Figure 5B presents the quenching data as a function of the [TRITC-$FlhA_C$]/[FITC-$FlhB_C$] ratio, normalized to a TRITC/$FlhA_C$ ratio of 1 (this normalization was carried out in all cases where the label/protein ratio (Table 2) was <1; see Experimental Procedures).

At the maximum [TRITC-$FlhA_C$]/[FITC-$FlhB_C$] ratio of 6 (corresponding to TRITC-$FlhA_C$ and FITC-$FlhB_C$ concentrations of 1.5 and 0.25 μM, respectively), the extent of quenching on this normalized scale was about 40%. Thus there clearly was association between $FlhA_C$ and $FlhB_C$. To explore the nature of the binding interactions, the same experiment was carried out in buffer containing either 0.5 M NaCl or 30% (v/v) 2-propanol (*i*PrOH) (Figure 5B). Quenching was not significantly affected by the presence of 0.5 M NaCl. However, 2-propanol caused some increase in fluorescence quenching.

Since it has been suggested that a $FlhA_C$−$FlhB_C$−FliH−FliI−FliJ−substrate complex may form during the export process (*5*), the impact of FliH and FliI on the interaction between $FlhA_C$ and $FlhB_C$ was also examined at a [TRITC-$FlhA_C$]/[FITC-$FlhB_C$] ratio of 1 (absolute concentrations of 0.25 μM). Over a range of FliH or FliI from 0 to 1.5 μM, neither protein significantly affected the energy transfer between TRITC-$FlhB_C$ and TRITC-$FlhA_C$ (data not shown).

$FlhA_C$−$FlhA_C$ and $FlhB_C$−$FlhB_C$ Interactions. The interactions of $FlhA_C$ with itself and of $FlhB_C$ with itself were also studied by FRET. The fluorescence intensity of FITC-$FlhA_C$ was quenched by the addition of TRITC-$FlhA_C$ (Figure 5C), reaching an extent of about 30% at a [TRITC-$FlhA_C$]/[FITC-$FlhA_C$] ratio of 6. NaCl caused a small increase in quenching, while 2-propanol caused a substantial decrease.

In similar experiments with FITC-$FlhB_C$ and TRITC-$FlhB_C$, fluorescence quenching was again observed (Figure 5D), in this case reaching an extent of 17% at a [TRITC-$FlhB_C$]/[FITC-$FlhB_C$] ratio of 6. Again, NaCl had little effect on the quenching, but 2-propanol caused a large increase.

Interactions between $FlhA_C$, FliH, and FliI and between $FlhB_C$, FliH, and FliI. FRET was also used to look for evidence for interactions between $FlhA_C$, FliH, and FliI and between $FlhB_C$, FliH, and FliI.

TRITC-FliH caused quenching of fluorescence intensity of FITC-$FlhA_C$. At a TRITC-FliH concentration of 1.5 μM, the extent of quenching was about 35% (Figure 6A). Effects of NaCl and 2-propanol were small.

In the case of FliI (whether wild-type or mutant) the label/protein ratio was always >1 (Table 2). We were uncertain of the validity of normalizing such data and therefore present unnormalized data. The quenching effect of TRITC-FliI on FITC-$FlhA_C$ was very pronounced, reaching a value of 51% at a TRITC-FliH concentration of 1.5 μM (Figure 6B). Both NaCl and 2-propanol reduced quenching appreciably.

The effects on $FlhB_C$ were very similar to those just described for $FlhA_C$, with TRITC-FliH (Figure 6C) giving substantial quenching (32% at a TRITC-FliH concentration of 1.5 μM). Effects of NaCl and 2-propanol were minor.

TRITC-FliI gave pronounced quenching of fluorescence of FITC-$FlhB_C$ (52% at a TRITC-FliI concentration of 1.5 μM, Figure 6D). Effects of NaCl and 2-propanol were much less pronounced than in the case of $FlhA_C$.

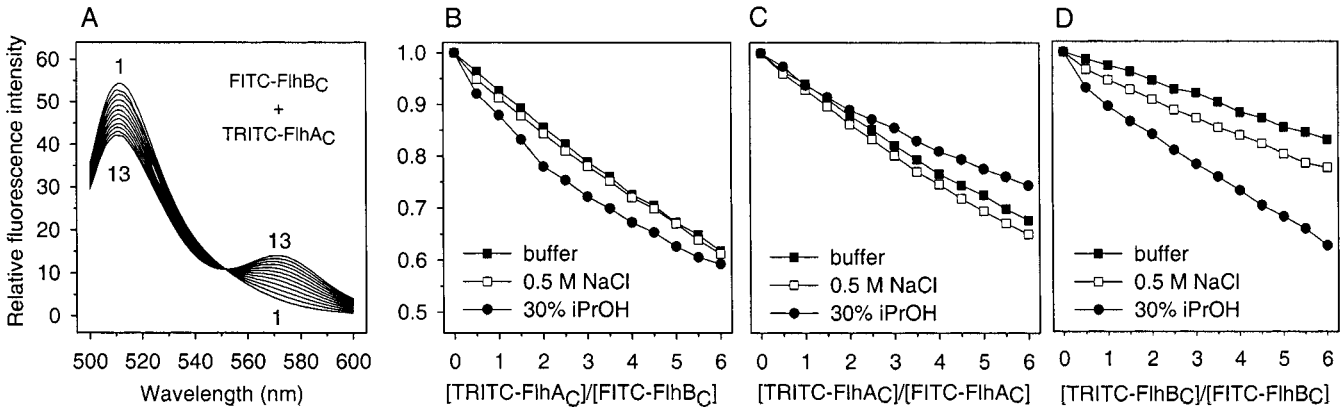

FIGURE 5: (A) Fluorescence spectra at 25 °C of FITC-FlhB_C plus TRITC-FlhA_C in 20 mM Hepes and 0.1 mM EDTA, pH 7.0. The FITC-FlhB_C concentration was 0.25 μM. The TRITC-FlhA_C concentration in spectra 1 through 13 was increased from 0 to 1.5 μM in 0.125 μM increments. The excitation wavelength was 494 nm, and both excitation and emission band-passes were 2 nm. (B) Quenching by TRITC-FlhA_C of the fluorescence of FITC-FlhB_C measured at 516 nm, as a function of [TRITC-FlhA_C]/[FITC-FlhB_C] concentration ratio ([FITC-FlhB_C] = 0.25 μM) in buffer, 0.5 M NaCl, and 30% 2-propanol (*i*PrOH). (C) Quenching of the fluorescence of FITC-FlhA_C by TRITC-FlhA_C. (D) Quenching of the fluorescence of FITC-FlhB_C by TRITC-FlhB_C. All spectra have been normalized to a TRITC/protein ratio of 1 (see Experimental Procedures and Results).

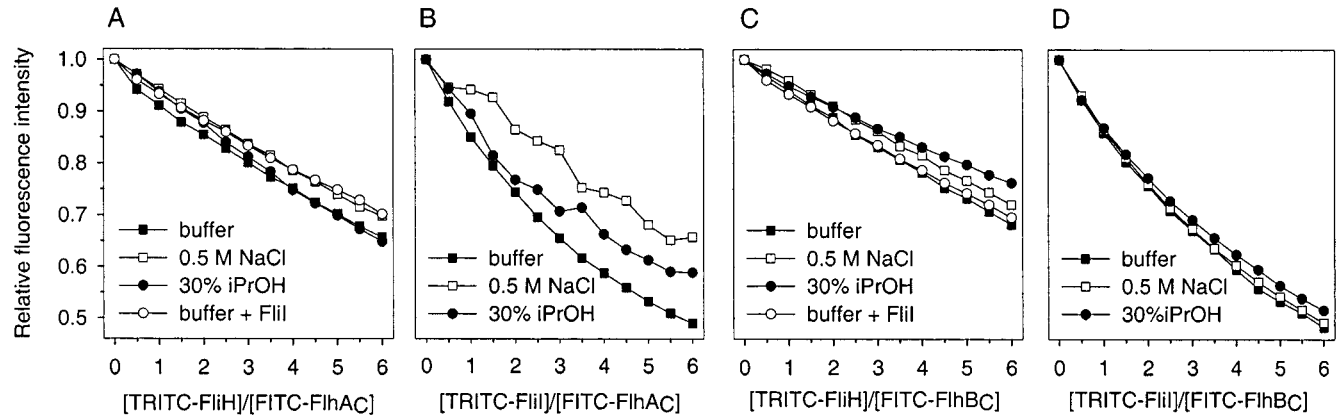

FIGURE 6: (A) Quenching of the fluorescence of FITC-FlhA_C by TRITC-FliH in buffer, 0.5 M NaCl, 30% 2-propanol, and buffer + 0.5 μM unlabeled FliI. (B) Quenching of the fluorescence of FITC-FlhA_C by TRITC-FliI. (C) Quenching of the fluorescence of FITC-FlhB_C by TRITC-FliH. (D) Quenching of the fluorescence of FITC-FlhB_C by TRITC-FliI. Spectra in (A) and (C) have been normalized to a TRITC/protein ratio of 1; those in (B) and (D) have not been normalized.

The presence of unlabeled wild-type FliI had little effect on the quenching of FITC-FlhA_C or FITC-FlhB_C fluorescence by TRITC-FliH (panels A and C of Figure 6).

Effects of FliH and FliI Mutations on Interactions with FlhA_C and FlhB_C. The interactions between FlhA_C, FlhB_C, and various mutant forms of FliH and FliI were also examined. In the case of FliH, the mutations were 10 amino acid deletions (FliHΔ1, FliHΔ3, FliHΔ4, FliHΔ5, FliHΔ6, and FliHΔ15) generated in another study (*18*). (The terminology means that, for example, FliHΔ1 is missing amino acids 1−10.) FliHΔ2 was not examined because it is insoluble.

Most of the TRITC-labeled mutant FliH proteins quenched the fluorescence intensity of FITC-FlhA_C less effectively than TRITC-labeled wild-type FliH, but the effects were not large (Figure 7A). With FITC-FlhB_C, the effects were even less pronounced (Figure 7C).

The FliI mutant proteins are ones that we have used previously (*1*). One of them has a double mutation (R7C/12P) near the N terminus and affects binding to FliH; the other two (K188I, Y363S) have catalytic mutations in the C-terminal domain. For both FITC-FlhA_C (Figure 7B) and FITC-FlhB_C (Figure 7D), these mutant proteins gave either similar quenching levels compared to wild-type FliI or slightly reduced levels.

Interactions between FliH and Wild-Type FliI and FliI (R7C/L12P). FliH and wild-type FliI form a $(FliH)_2FliI$ complex (*16*, *17*). In a previous study, interaction of FliH with wild-type FliI was readily detected by Ni-NTA chromatography; interaction of FliH with mutant FliI (R7C/L12P), however, was not detected, indicating that the N terminus of FliI is important for association with FliH (*16*). We examined this question by FRET (Figure 8) and found that although TRITC-FliI (R7C/L12P) did quench FITC-FliH fluorescence to some degree (and therefore must have had some capacity to interact with FliH), it did so much less effectively than TRITC-labeled wild-type FliI.

DISCUSSION

Previous work concerning the flagellar protein export system has mostly concerned its soluble components. The goal of the present study was to gain some understanding of interactions involving membrane components of the system. We used two different types of techniques. The first were biochemical (affinity chromatography and affinity blotting) and were applied to two full-length membrane proteins, FlhA

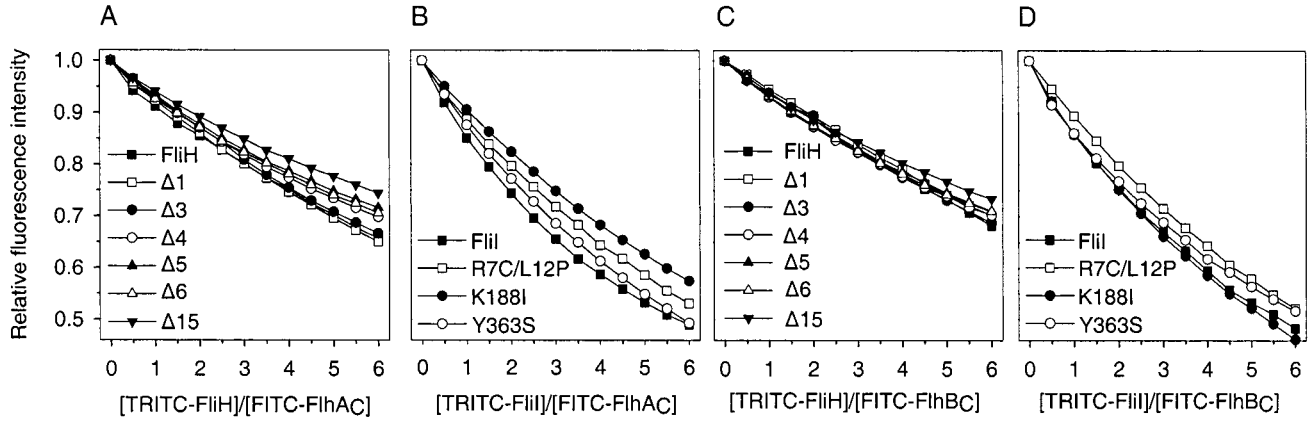

FIGURE 7: (A) Quenching of the fluorescence of FITC-FlhA_C by TRITC-labeled deletion mutant forms of FliH (TRITC-FliHΔ1, etc.). (B) Quenching of the fluorescence of FITC-FlhA_C by TRITC-labeled mutant forms of FliI. (C) Quenching of the fluorescence of FITC-FlhB_C by TRITC-labeled deletion mutant forms of FliH. (D) Quenching of the fluorescence of FITC-FlhB_C by TRITC-labeled mutant forms of FliI. Spectra in (A) and (C) have been normalized to a TRITC/protein ratio of 1; those in (B) and (D) have not been normalized.

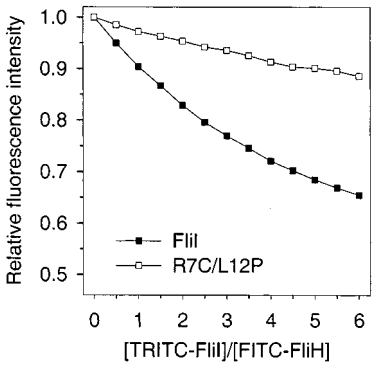

FIGURE 8: Quenching of the fluorescence of FITC-FliH by TRITC-wild-type-FliI and by TRITC-FliI (R7C/L12P). Spectra have not been normalized.

and FlhB. However, we also found that study of the soluble C-terminal domains (FlhA_C and FlhB_C) could provide useful information, and we made extensive use of fluorescence resonance energy transfer (FRET) for this purpose. We also examined wild-type and mutant versions of FliI (the export ATPase) and FliH (negative regulator of FliI), with respect to interactions with FlhA_C and FlhB_C.

Interactions between FlhA and FlhB. Affinity chromatography and affinity blotting data indicated interactions between FlhA and FlhB. Since both FlhA and FlhB have hydrophobic transmembrane domains, it is possible that the interactions between them are nonspecific. However, in equivalent experiments, we failed to find evidence for FlhA−FlhA or FlhB−FlhB interactions, supporting the contention that the FlhA−FlhB interactions are specific.

In FRET measurements, we observed not only heterologous interactions between FlhA_C and FlhB_C (Figure 5A,B) but also homologous interactions, FlhA_C−FlhA_C (Figure 5C) and FlhB_C−FlhB_C (Figure 5D). There could be two reasons for the difference between the affinity measurements and the FRET measurements: the sensitivity of the techniques used and the presence versus the absence of the membrane domain. In a previous study (*5*), affinity blotting indicated only weak interactions between FlhA_C and FlhA_C, FlhB_C and FlhB_C, and FlhA_C and FlhB_C. However, affinity blotting is dependent on substantial refolding of the target protein on the membrane, while the FRET experiments were carried out in solution, using a buffer that approximated physiological conditions. We conclude that the FRET data are more sensitive and that FlhA and FlhB interact in both a heterologous and a homologous fashion.

FliH and FliI did not have a major effect on the energy transfer from FITC-FlhB_C to TRITC-FlhA_C and so presumably do not change the FlhA_C−FlhB_C binding interactions.

Interaction of FlhA_C and FlhB_C with FliH and FliI. The FRET results indicate that both FlhA_C and FlhB_C bind FliH and FliI. This is in general agreement with data from affinity blotting where FlhA_C or FlhB_C was the probe and FliH or FliI was the target; however, as was noted, evidence for interactions was much weaker where FlhA_C or FlhB_C was the target (*5*), presumably indicating that these molecules did not fully renature on the membrane. We conclude that, under the physiological buffer conditions of our FRET measurements, FlhA_C and FlhB_C do bind both FliH and FliI.

Effects of Mutations in FliH or FliI on Binding to FlhA_C and FlhB_C. The effects of mutations in FliH and FliI were small. In the case of FliH, some of the deletion mutations caused a decrease in quenching, especially with FlhA_C. There was a general trend that deletions further from the N terminus caused a greater decrease in quenching. We tentatively suggest that the N terminus of FliH plays a less important role than the rest of the FliH sequence in the interaction with FlhA_C. With FlhB_C, the effects of the FliH mutations were too small for any useful conclusions to be drawn.

In the case of FliI, all three of the mutations tested (both catalytic and structural) caused no decrease or only a small decrease in quenching of both FlhA_C and FlhB_C. Recall that these data were not normalized to the TRITC/protein ratio. Because the mutant FliI proteins had lower label levels than wild-type FliI (Table 2), normalized data (not shown) indicate that the mutant proteins bind more strongly than wild type to both FlhA_C and FlhB_C; we doubt, however, that this is actually the case and consider the unnormalized data more reliable.

Interactions between FliH and Wild-Type and Mutant FliI. The interactions between FliH and FliI have been studied extensively (*16*−*18*). Specifically, it is known that the N terminus of FliI is important for association with FliH. This knowledge then provided us with the opportunity to test the validity of the FRET method for determining association between components of the flagellar export system. We

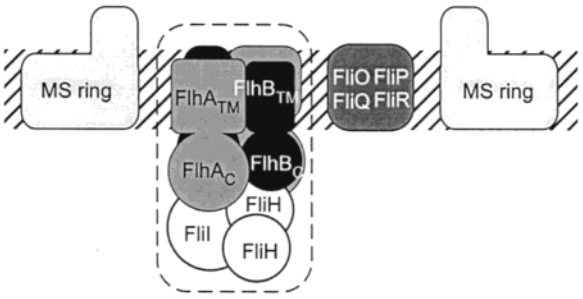

FIGURE 9: Cartoon of the membrane components of the flagellar protein export apparatus, depicting interactions between components observed in this study. The membrane-associated components are believed to lie in a specialized patch of membrane within a central pore in the basal body MS ring. Membrane outside and inside the MS ring is indicated by hatching. There are six membrane components, FlhA, FlhB, FliO, FliP, FliQ, and FliR. The latter four proteins were not a part of this study, and no conclusion should be drawn from the way they are depicted. The proteins that were studied are enclosed in the dashed outline: they are FlhA, FlhB (two copies of each shown), and the soluble proteins FliI (an ATPase) and FliH (a negative regulator of FliI), which form a heterotrimeric complex. Sizes approximate the actual molecular masses. FlhA and FlhB have large N-terminal transmembrane domains ($FlhA_{TM}$ and $FlhB_{TM}$) and large soluble C-terminal domains ($FlhA_C$ and $FlhB_C$). The existence of a heterotrimeric complex between FliI and FliH is well established (*16*−*18*). In the present study, we confirmed the FliH−FliI interaction and additionally established the following interactions: FlhA−FlhB, $FlhA_C$−$FlhB_C$, $FlhA_C$−$FlhA_C$, $FlhB_C$−$FlhB_C$, FliH−$FlhA_C$, FliH−$FlhB_C$, FliI−$FlhA_C$, and FliI−$FlhB_C$. We were unable to detect interactions between intact FlhA and itself or between intact FlhB and itself.

found that energy transfer between FITC-FliH and TRITC-FliI (R7C/L12P) was indeed poor (about 3-fold) compared with that between FITC-FliH and TRITC-labeled wild-type FliI (Figure 8). We take this as a validation of the FRET method. It is interesting that the energy transfer with FliI (R7C/L12P) was not zero, indicating the capability of FRET to detect weak interactions that escaped detection by other methods. Corroborating the FRET result is the fact that a *fliI* null mutant transformed with a plasmid overproducing FliI (R7C/L12P) does show weak motility (*1*).

Nature of the Interactions Observed. Fluorescence energy transfer is strongly related (inversely dependent on r^6) to the distance between donor and acceptor (*27*). Changes in fluorescence quenching as a function of the buffer used are therefore an indication of weaker or stronger interactions between the two species under study, as a result of either weaker binding or a more open complex, and can suggest the nature of the interaction between them. In addition to simple buffer, we tested the effects of high salt (0.5 M NaCl) and increased hydrophobicity (30% 2-propanol). A decrease in quenching at high salt suggests that electrostatic interactions are important, whereas an increase suggests that hydrophobic interactions are important. A decrease in quenching at higher hydrophobicity suggests that hydrophobic interactions are important (*28*), whereas an increase suggests that electrostatic and/or hydrogen-bonding interactions are important.

Although we observed significant changes in quenching in many instances, we will restrict our comments to the situations where the largest effects were observed. The first was the effect on $FlhA_C$−$FlhB_C$ interactions, where 2-propanol caused an increase in quenching (Figure 5B), suggesting that the interface is dominated by electrostatic and/or hydrogen-bonding interactions. The second was the effect on $FlhA_C$−$FlhA_C$ interactions, where 2-propanol caused a decrease in quenching (Figure 5C), suggesting that the $FlhA_C$−$FlhA_C$ interface is substantially hydrophobic. The third was the effect on $FlhB_C$−$FlhB_C$ interactions, where 2-propanol caused a large increase in quenching (Figure 5D), suggesting that the interface is dominated by electrostatic and/or hydrogen-bonding interactions. The fourth was the effect on FliI−$FlhA_C$ interactions, where 2-propanol and high salt both caused reduced quenching, suggesting that hydrophobic and electrostatic and/or hydrogen-bonding interactions are all important.

Proposed Model for the Export Apparatus Complex. A model summarizing the interactions we have established is given in Figure 9. Although our measurements were pairwise ones, we suspect they reflect the existence, whether dynamic or stable, of a complex consisting of FlhA, FlhB, FliH, and FliI. Whether FliO, FliP, FliQ, and FliR are also part of this complex remains to be established.

We do not envisage that, in the context of the complete membrane complex of the export apparatus within the pore of the MS ring, there are large assemblages of FlhA and FlhB, because spatial restrictions preclude that possibility. We have estimated previously that the available space within the pore could accommodate around 70 membrane-spanning α helices (*2*). With FlhA at eight predicted spans (*12*) and FlhB at four (*13*) [in addition to FliO at one, FliP at three or four, FliQ at two, and FliR at five or six (*3*)], we suspect the stoichiometries of those proteins with a large number of spans (FlhA, FlhB, FliP, and FliR) will be small. A $(FlhA)_2$-$(FlhB)_2$ heterotetramer contributing to the total complex could be a reasonable possibility.

ACKNOWLEDGMENT

We thank Andrew Miranker for use of his spectrofluorometer and May Kihara for plasmid constructions.

REFERENCES

1. Fan, F., and Macnab, R. M. (1996) *J. Biol. Chem. 271*, 31981−31988.
2. Fan, F., Ohnishi, K., Francis, N. R., and Macnab, R. M. (1997) *Mol. Microbiol. 26*, 1035−1046.
3. Ohnishi, K., Fan, F., Schoenhals, G. J., Kihara, M., and Macnab, R. M. (1997) *J. Bacteriol. 179*, 6092−6099.
4. Minamino, T., and Macnab, R. M. (1999) *J. Bacteriol. 181*, 1388−1394.
5. Minamino, T., and Macnab, R. M. (2000) *Mol. Microbiol. 35*, 1052−1064.
6. Minamino, T., Chu, R., Yamaguchi, S., and Macnab, R. M. (2000) *J. Bacteriol. 182*, 4207−4215.
7. Fraser, G. M., Bennett, J. C. Q., and Hughes, C. (1999) *Mol. Microbiol. 32*, 569−580.
8. Auvray, F., Thomas, J., Fraser, G. M., and Hughes, C. (2001) *J. Mol. Biol. 308*, 221−229.
9. Yokoseki, T., and Kutsukake, K. (1994) *Jpn. J. Genet. 69*, 778.
10. Katayama, E., Shiraishi, T., Oosawa, K., Baba, N., and Aizawa, S.-I. (1996) *J. Mol. Biol. 255*, 458−475.
11. Suzuki, H., Yonekura, K., Murata, K., Hirai, T., Oosawa, K., and Namba, K. (1998) *J. Struct. Biol. 124*, 104−114.
12. Kihara, M., Minamino, T., Yamaguchi, S., and Macnab, R. M. (2001) *J. Bacteriol. 183*, 1655−1662.
13. Williams, A. W., Yamaguchi, S., Togashi, F., Aizawa, S.-I., Kawagishi, I., and Macnab, R. M. (1996) *J. Bacteriol. 178*, 2960−2970.
14. Minamino, T., and Macnab, R. M. (2000) *J. Bacteriol. 182*, 4906−4914.

15. Vogler, A. P., Homma, M., Irikura, V. M., and Macnab, R. M. (1991) *J. Bacteriol. 173*, 3564−3572.
16. Minamino, T., and Macnab, R. M. (2000) *Mol. Microbiol. 37*, 1494−1503.
17. Minamino, T., Tame, J. R. H., Namba, K., and Macnab, R. M. (2001) *J. Mol. Biol. 312*, 1029−1037.
18. González-Pedrajo, B., Fraser, G. M., Minamino, T., and Macnab, R. M. (2002) *Mol. Microbiol.* (in press).
19. Minamino, T., Iino, T., and Kutsukake, K. (1994) *J. Bacteriol. 176*, 7630−7637.
20. Kõiv, A., Palvimo, J., and Kinnunen, P. K. J. (1995) *Biochemistry 34*, 8018−8027.
21. Jameson, D. M., and Seifried, S. E. (1999) *Methods 19*, 222−233.
22. Haugland, R. P. (1999) *Handbook of Fluorescent Probes and Research Chemicals*, 7th ed., Molecular Probes, Eugene, OR.
23. Bateson, M., Devenish, R. J., Nagley, P., and Prescott, M. (1999) *J. Biol. Chem. 274*, 7462−7466.
24. Vanderkooi, J. M., Lerokomar, A., Nakamura, H., and Martinosi, A. (1977) *Biochemistry 16*, 1262−1267.
25. Sharma, N., Hewett, J., Ozelius, L. J., Ramesh, V., McLean, P. J., Breakefield, X. O., and Hyman, B. T. (2001) *Am. J. Pathol. 159*, 339−344.
26. Förster, T. (1948) *Ann. Phys. (Leipzig) 2*, 55−75.
27. Lakowicz, J. R. (1999) *Principles of Fluorescence Spectroscopy*, 2nd ed., Plenum, New York.
28. Rosell, C. M., Vaidya, A. M., and Halling, P. J. (1995) *Biochim. Biophys. Acta 1252*, 158−164.

BI0203280